

# Emergence of Order in Textured Patterns

Gemunu H. Gunaratne<sup>1,2</sup>, Anuradha Ratnaweera<sup>2</sup> and K. Tennekone<sup>2</sup>

<sup>1</sup> *Department of Physics, The University of Houston, Houston, TX 77204*

<sup>2</sup> *The Institute of Fundamental Studies, Kandy, Sri Lanka*

A characterization of textured patterns, referred to as the disorder function  $\bar{\delta}(\beta)$ , is used to study properties of patterns generated in the Swift-Hohenberg equation (SHE). It is shown to be an intensive, configuration-independent measure. The evolution of random initial states under the SHE exhibits two stages of relaxation. The initial phase, where local striped domains emerge from a noisy background, is quantified by a power law decay  $\bar{\delta}(\beta) \sim t^{-\frac{1}{2}\beta}$ . Beyond a sharp transition a slower power law decay of  $\bar{\delta}(\beta)$ , which corresponds to the coarsening of striped domains, is observed. The transition between the phases advances as the system is driven further from the onset of patterns, and suitable scaling of time and  $\bar{\delta}(\beta)$  leads to the collapse of distinct curves.

The decay of  $\bar{\delta}(\beta)$  during the initial phase remains unchanged when nonvariational terms are added to the underlying equations, suggesting the possibility of observing it in experimental systems. In contrast, the rate of relaxation during domain coarsening increases with the coefficient of the nonvariational term.

## I. INTRODUCTION

The study of spatio-temporal patterns has received considerable impetus from a series of elegant experiments and theoretical developments based on symmetry considerations. Recent experimental studies include those on reaction diffusion chemical systems [1], convection in fluids [2] and gases [3], ferrofluids [4], and vibrated layers of granular material [5]. These results have been supplemented with patterns generated in (relatively) simple model systems [6–8]. The most complete theoretical treatments of patterns rely on the study of symmetries of the underlying system and those of the patterns [9]. Unfortunately, this analysis is restricted to periodic or quasi-periodic patterns. A theoretical analysis of more complex states requires the identification of suitable “variables” to describe a given pattern. Examples of such variables include the structure factor [10], the correlation length [11–13] and the density of topological defects [14]. In this paper we study properties of another characterization, referred to as the “disorder function” [15,16].

The patterns studied are generated in physical systems (and models) whose control parameters are uniform in space and time; thus, they result from spontaneous symmetry breaking. The simplest class of nontrivial structures are periodic. They are typically striped, square, triangular or hexagonal patterns that form in perfect, extended arrays [6]. To obtain periodic patterns, the initial state of the system and/or the boundary conditions need to be carefully prepared. A second class consist of periodic patterns whose “unit cells” have additional structure [17,18]. A field describing periodic arrays can be expanded in a few plane waves.

The patterns described above contain a unit cell that is repeated on a “Bravais lattice” to generate a plane-filling structure. The qualitative description of the pattern in-

volves the characterization (in terms of symmetries) of the unit cell and the generators of the Bravais lattice. For example, the unit cell of a honeycomb lattice is  $D_6$ -symmetric, and the Bravais lattice is generated by two unit vectors  $120^\circ$  apart.

Quasi-periodic patterns have also been observed under suitable experimental conditions [19]. Their symmetries can be observed in Fourier space. For example, the spectrum of a quasi-crystal is 10-fold symmetric [20]. Quasi-periodic patterns can be described using a few “principal” plane waves along with their nonlinear couplings.

The bifurcations to and from a given periodic (or quasi-periodic) state can be studied using the “Landau equations,” which once again rely on the symmetries of the physical system and the pattern [21]. The information used is that, since the pattern is generated by symmetry breaking, a second pattern obtained under the action of any symmetry of the *physical system* has identical features. The imposition of this equivalence (supplemented by the elimination of “higher order” terms) gives the normal form equations of the pattern. They contain information on aspects of dynamics of the pattern and details about its bifurcations [9].

Patterns such as those of Figs. 1 and 2 (which are generated in a model system) do not belong to the classes discussed above. These structures, referred to as “textured” or “natural” patterns [22], are observed when the initial states from which they evolve are not controlled. Similar structures are seen in small aspect ratio systems when the boundaries play a significant role in the creation of the pattern [6].

There is no (nontrivial) global symmetry of textures; consequently, they cannot be characterized using symmetry groups. Note also that a second realization of the experiment (e.g., starting from a different set of initial conditions) will give a pattern that is vastly different in

detail (such as Figs. 1(a) and 1(b)). In spite of these differences, one can clearly recognize similarities between distinct patterns. For example, the correlation length and the density of topological defects of the two textures shown in Fig. 1 are similar. In contrast patterns generated under other external conditions (e.g., Fig. 2) have different characteristics. A theoretical treatment of textured patterns requires a “configuration independent” description.

FIG. 1. Two patterns generated by evolving random initial states via the Swift-Hohenberg equation for 1600 time units. The parameters used were  $D = 0.1$ ,  $\epsilon = 0.2$ ,  $\nu = 2$  and  $k_0 = 1$ . The initial states consisted of white noise whose intensity varied between 0 and  $10^{-3}$ . Periodic boundary conditions were imposed on the square domain of  $256 \times 256$  lattice points, the length of whose sides are  $(48\pi/k_0)$ .

In Section II, we introduce the disorder function  $\bar{\delta}(\beta)$  whose definition was motivated in part by the argument leading to the derivation of Landau equations; for patterns generated in uniform, extended systems,  $\bar{\delta}(\beta)$  is required to be invariant under rigid motions of a labyrinthine pattern [15,16]. In section III, we briefly describe the method for evaluating the disorder function from (typically noisy) grid-values of the field. It relies on a method to approximate a continuous function from values given on a grid referred to as the method of “Distributed Approximating Functionals” (DAFs) [23].

The main results of the paper, which include properties of the disorder function, and its application to provide a quantitative description of the relaxation of the patterns from an initially random state are presented in Sections IV and V. The underlying spatio-temporal dynamics is given by the Swift-Hohenberg equation (SHE) and one of its variants. We first provide evidence to support the claim that the disorder function consists of intensive, configuration independent variables. The use of  $\bar{\delta}(\beta)$  shows that pattern relaxation occurs in two distinct phases separated by a sharp transition. We also study changes in the relaxation profile when the system is driven further away from the onset of patterns. In Section V, we discuss the effects of adding nonvariational terms to the SHE.

FIG. 2. Two patterns generated by evolving a random initial state via the Swift-Hohenberg equation for 2400 time units. The parameters used for the integration were  $D = 0.01$ ,  $\epsilon = 0.4$ ,  $\nu = 2$  and  $k_0 = 1/3$ . The initial states consisted of white noise whose intensity varied between  $\pm 10^{-2}$ . The length of each side of the square is  $(48\pi/k_0)$ .

## II. THE DISORDER FUNCTION

Textured patterns observed in experimental systems [1–5] and those shown in Figs. 1 and 2 can be described by a scalar field  $v(\mathbf{x})$  which is smooth, except perhaps at

the defect cores. However, unless the patterns are trivial (e.g., perfect stripes, target patterns) the analytical form of the field is unknown. Consequently, it is difficult to determine a set of “configuration independent” characteristics of structures generated under similar conditions. We instead impose a weaker requirement, that the characterizations remain invariant under the action of the symmetries of the underlying physical system; i.e., translations, rotations and reflections [15]. Rather surprisingly, the measures so defined have similar values for distinct patterns such as those shown in Fig. 1.

The most significant feature of labyrinthine patterns is that they are locally striped; in a suitable neighborhood  $v(\mathbf{x}) \sim \sin(\mathbf{k} \cdot \mathbf{x})$ , where the modulus  $k_0 (\equiv |\mathbf{k}|)$  of the wave vector does not vary significantly over the pattern. Structures generated in experiments and model systems include higher harmonics due to the presence of nonlinearities in the underlying system; they only contribute to the shape of the cross section of stripes. In order to use the simplest characterization of textures, we eliminate the second and higher order harmonics by the use of a suitable window function in Fourier space. For experimental patterns (which do not have periodic boundary conditions) this is a nontrivial task, and a method to implement it is described in Ref. [24].

The simplest local field that is derived from  $v(\mathbf{x})$  and whose value remains the same under all rigid motions is its Laplacian  $\Delta v(\mathbf{x})$ . Terms such as  $\Delta^n v^m(\mathbf{x})$ , though invariant, are difficult to extract from an incompletely sampled field (typically given on a square lattice). The requirement that perfect stripes be assigned a null measure (they are not disordered), coupled with the local sinusoidal form of the (filtered) pattern implies that the lowest-order field relevant for our purpose is  $(\Delta + k_0^2)v(\mathbf{x})$ . The family of measures, referred to as the disorder function, is defined by

$$\delta(\beta) = (2 - \beta) \frac{\int da |(\Delta + k_0^2)v(\mathbf{x})|^\beta}{k_0^{2\beta} \langle |v(\mathbf{x})| \rangle^\beta}, \quad (1)$$

where  $\langle |v(\mathbf{x})| \rangle$  denotes the mean of  $|v(\mathbf{x})|$ , and  $\delta(\beta)$  has been normalized so that the “intensive variables”  $\bar{\delta}(\beta) = \delta(\beta) / \int da$  are scale invariant. The moment  $\beta$  is restricted to lie between 0 and 2 for reasons discussed below. Local deviations of the patterns from stripes (due to curvature of the contour lines [15]) contribute to  $\delta(\beta)$  through the Laplacian, while variations of the width of the stripes contribute via the choice of a “global”  $k_0$ .

$\bar{\delta}(\beta)$  depends on the choice of the wave-number  $k_0$  of the “basic” stripes. Analysis of striped patterns  $u_{st}(\mathbf{x}) = A \sin(\mathbf{k} \cdot \mathbf{x})$  and target patterns  $u_t(\mathbf{x}) = A \cos(kr)$  show that  $\bar{\delta}(1)$  is minimized when  $k_0 = k = |\mathbf{k}|$ . Studies of textured patterns from model equations indicate (see Fig. 3) the presence of a unique minimum of  $\bar{\delta}(1)$ . We use the minimization of  $\bar{\delta}(1)$  as the criterion for the choice of the wave-number  $k_0$  in Eqn. (1). For patterns generated us-

ing the Swift-Hohenberg equation [6],  $k_0$  is very close to the wave-number obtained by minimizing the “energy” [25]. We also find that our estimation of  $k_0$  is far more robust (i.e., smaller variation between distinct patterns) than that evaluated from the power spectrum. This is presumably because wavelength variations and curvature of contour lines at each location of the pattern contribute to the computation of  $\bar{\delta}(\beta)$ .

The variation in  $k$  over the pattern (traditionally defined to be the half width of the Structure Factor [27]) can be estimated using the variation of  $\bar{\delta}(1)$  with the wave-number  $k$  (see Fig. 3). In the remainder of the paper we define  $\Delta k$  to be the distance between  $k$ -values for which  $\bar{\delta}(1)$  is twice the minimum value [26]. Analysis of textures shows that  $\Delta k$  is a configuration-independent, intensive variable.

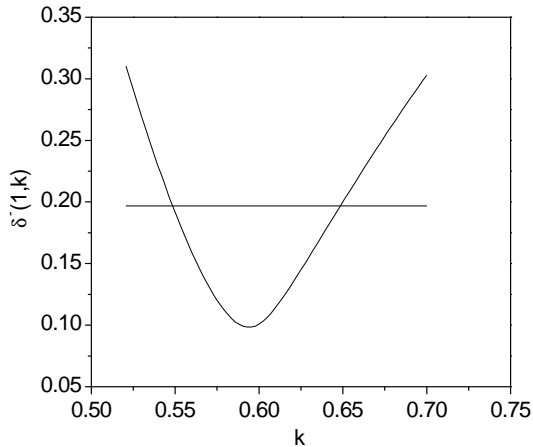


FIG. 3. The behavior of  $\bar{\delta}(1)$  as a function of the wave-number  $k$  for a labyrinthine pattern.  $k_0$  is estimated to be the (unique) minimum of the curve. The width  $\Delta k$  is defined to be the distance between the  $k$ -values at which  $\bar{\delta}(1)$  reaches twice its minimum.

Observe that our choice of  $k_0$  is arbitrary in one sense; we could have chosen to minimize  $\bar{\delta}(\beta)$  for any fixed  $\beta$  to determine  $k_0$ . However, the observed variations in  $k_0$  are insignificant. Alternatively, we could have evaluated *each*  $\bar{\delta}(\beta)$  by minimizing it with respect to  $k$ . We choose not to implement this scheme because of the need to estimate only one free parameter (i.e., the wave-number) for a given pattern.

For a perfect set of stripes the function  $\bar{\delta}(\beta) = 0$ . A

domain wall contains curvature of the contour lines and variations of the stripe width; consequently it has non-zero disorder.  $\delta(\beta)$  for a single domain wall is a monotonically increasing function of the angle  $\theta$  between the stripes of the two domains [28]. Thus  $\delta(\beta)$  provides information absent in characterizations such as the correlation length. The disorder function for a target pattern  $v(\mathbf{x}) = a \cos(k_0 r)$  is known [15], and is used to determine the accuracy of the numerical algorithms. For target patterns, the integral in the numerator diverges as  $(2 - \beta)^{-1}$ , and leads to limiting the range of  $\beta (< 2)$ , and to the introduction of the prefactor in the definition of  $\delta(\beta)$ .

The weights of distinct characteristics of a texture (e.g., domain walls, defects, variations of the stripe-width, etc.) depend on the moment  $\beta$ . In particular, the contribution to  $\delta(\beta)$  from a domain wall vanishes as  $\beta \rightarrow 2$ , and the limit is proportional to the number of targets in a pattern. The effects of noise on the calculations are minimal. For example, addition of 10% white noise typically changes  $\delta(\beta)$  by less than 2%.

### III. DISTRIBUTED APPROXIMATING FUNCTIONALS

The critical requirement for a good estimate of  $\bar{\delta}(\beta)$  is a sufficiently accurate determination of the Laplacian. Calculation of derivatives of a field from values given on a lattice is a delicate task, especially in the presence of noise. A technique, utilizing what are referred to as Distributed Approximating Functionals (DAFs), has been introduced recently, to fit analytically or approximate a continuous function from known values on a discrete grid [23]. Unlike typical finite difference schemes, it estimates the function and its derivatives using a range of neighboring points ( $\sim 40$  in our case); consequently, the required computations are much less sensitive to noise.

The most useful for our application has been a class of DAFs for which the order of accuracy of the fit is the same both on and off the grid. (This is in contrast to interpolation, which forces the fit to be exact on the grid, but always leads to intertwining about the function off the grid, thus leading to less accurate estimation of derivatives.) Alternatively, the method is designed so that there are no special points. If the labels on the grid points are erased after DAF-fitting of a function, it becomes essentially impossible to identify the points that were on the grid. The most general derivation of the DAFs is via a variational principle [29], yielding

$$g_{DAF}(x) = \sum_k I(x, x_k) g(x_k), \quad (2)$$

where  $k$  labels the grid points,  $g(x_k)$  are the known input values of the function (which may contain noise), and the sum is over  $x_k$  such that  $|x_k - x|/\Delta < R$ ,  $\Delta$  being the lattice spacing. For suitable  $I(x, x_k)$ , the function and

its derivatives are evaluated to a comparable accuracy [29]. This proves crucial in the evaluation of the disorder function.

The calculations presented are carried out using the ‘‘Hermite DAF’’ [30], defined by

$$I(x, x_k) = I(x - x_k) = \frac{\Delta}{\sigma} \frac{e^{-z^2}}{\sqrt{2\pi}} \sum_{j=0}^{M/2} \left(-\frac{1}{4}\right)^j \frac{1}{j!} H_{2j}(z), \quad (3)$$

where  $z = (x - x_k)/\sigma\sqrt{2}$  and  $H_n(z)$  is the  $n^{\text{th}}$  Hermite polynomial. The Gaussian weight (of width  $\sigma$ ) in Eqn. (3) makes  $I(x_l - x_k)$  highly banded, reducing the computational cost of applying the DAF to data. The DAF representation of derivatives of a function known only on a grid is given by

$$\left(\frac{d^l g}{dx^l}\right)_{DAF}(x) = \sum_k \frac{d^l}{dx^l} I(x, x_k) g(x_k), \quad (4)$$

which can be evaluated either on or off the grid. In the continuum limit, the derivative of the DAF equals (exactly) the DAF of the derivative [30].

The DAF approximation to a function that is sampled on a square grid  $(x_m, y_n)$  can be obtained using the two-dimensional extension

$$I((x, y), (x_m, y_n)) = I_X(x, x_m) I_Y(y, y_n) \quad (5)$$

of the approximating kernel [31]. Thus to estimate (say)  $\frac{d^2 v}{dx^2}$ , Eqn. (4) needs to be applied in the  $y$ -direction (with  $l = 0$ ) and along the  $x$ -direction (with  $l = 2$ ). (The application of the DAF operators in the two directions commute and can be carried out in any order.)

As  $M \rightarrow \infty$ ,  $I(x, x_k) \rightarrow \delta(x - x_k)$ , and the DAF approximation  $g_{DAF}(x)$  becomes exact. With finite  $M$ , the sum on the right side of Eqn. (3) becomes a polynomial (of order  $M$ ), resulting in  $g_{DAF}(x)$  being smooth. Note that  $g_{DAF}(x)$  can be considered to be a weighted running average of the signal. The Gaussian width  $\sigma$  determines the effect of neighboring points in the DAF-approximation. The range  $R$  is chosen to be sufficiently large that the terms ignored in Eqn. (2) are negligible. (The Gaussian weight included in the definition of  $I(x, x_k)$  guarantees the decay of these terms.)

#### IV. PATTERNS GENERATED USING THE SWIFT-HOHENBERG EQUATION

The patterns analyzed in the paper are obtained from periodic fields  $u(\mathbf{x}, t)$  generated by integrating random initial states through a modified Swift-Hohenberg equation (SHE) [32,6]

$$\partial_t u = D\left(\epsilon - (k_0^2 + \Delta)^2\right)u - \gamma u^3 - \nu(\nabla u)^2. \quad (6)$$

The parameters  $D$ ,  $k_0$ , and  $\gamma$  can be eliminated through suitable rescaling of  $t$ ,  $\mathbf{x}$ , and  $u$  respectively.  $\epsilon$  measures the distance from the onset of patterns. The results for the variational case ( $\nu = 0$ ) are presented in this Section and those for the nonvariational case ( $\nu \neq 0$ ) are given in the next.

The initial fields for the integration were random numbers in a predetermined range. The time evolution is implemented using the Alternating Direction Implicit algorithm [34]. Each nonlinear term  $N[u(\mathbf{x}, t)]$  is expanded to first order in  $\delta u = u(\mathbf{x}, t + \delta t) - u(\mathbf{x}, t)$ , thus linearizing the equations in  $u(\mathbf{x}, t + \delta t)$ . Updating the field involves the inversion of a penta-diagonal matrix. The typical time step used for the integration,  $\Delta t \sim 0.1$ , was chosen so that the higher order terms in  $\delta u$  are insignificant. We have confirmed the robustness of the integration by comparing (in a few cases) the results with those done for a smaller time-step ( $\Delta t \sim 0.001$ ).

#### A. Properties of the disorder function

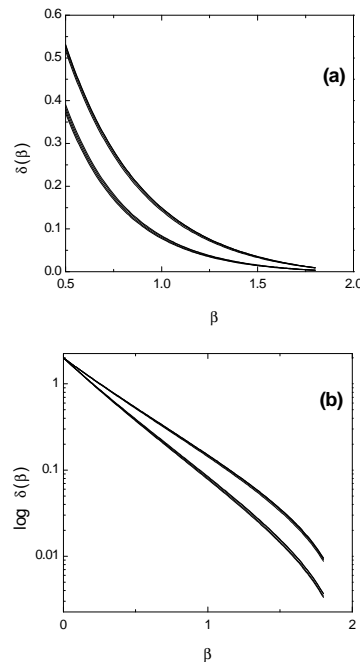


FIG. 4. The curves  $\bar{\delta}(\beta)$  for patterns generated at two different sets of control parameters. The lower bunch consists of curves for four patterns at the first set of control parameters (Fig. 1) while the upper bunch consist of those for a second set of control parameters (Fig. 2). (b) shows the same plots with a logarithmic vertical scale.

The form of the measures  $\bar{\delta}(\beta)$  were deduced by requiring invariance under rigid motions of a single pattern. *Are these limited restrictions sufficient to yield characterizations that can delineate the observed “commonality” in distinct patterns generated under identical conditions?* Surprisingly, it appears to be the case. Fig. 4 shows the disorder functions for several patterns. The curves bunched at the bottom show  $\bar{\delta}(\beta)$  for four textures (two of which are shown in Fig. 1) generated at fixed control parameters.  $\bar{\delta}(\beta)$  appears to have captured the commonality of these distinct patterns. Structures generated in the Gray-Scott model [33] and in a vibrated layer of granular material [5] exhibit similar properties [28].

The next question is if  $\bar{\delta}(\beta)$  can differentiate between patterns with different visual characteristics. Fig. 2 shows two structures obtained from the SHE for a second set of control parameters. They have characteristics that differ from patterns of Fig. 1; e.g., they contain smaller domains and a larger density of defects.  $\bar{\delta}(\beta)$  for four such textures are bunched together on the upper curves in Fig. 4. The significant separation of the two sets of curves (e.g., the values of  $\bar{\delta}(1)$  between the two sets is about 25 times larger than the average difference between curves within a set) confirms the ability of  $\bar{\delta}(\beta)$  to quantify the differences of the two groups of patterns.

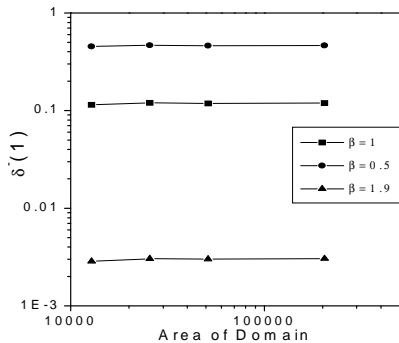


FIG. 5. The values of  $\bar{\delta}(0.5)$ ,  $\bar{\delta}(1.0)$  and  $\bar{\delta}(1.9)$  for periodic patterns generated in domains of different sizes. The areas of the domains are  $36\pi \times 36\pi$ ,  $36\pi \times 72\pi$ ,  $72\pi \times 72\pi$ , and  $144\pi \times 144\pi$ . In each case random initial states are evolved for 8000 time units under the SHE with control parameters given in Fig. 2. The results indicate that  $\bar{\delta}(\beta)$  are intensive variables for labyrinthine patterns.

The disorder function quantifies the characteristics of a labyrinthine pattern using the local curvature of the contour lines and the wavelength variations, which typically increase with the (visual) disorder of a texture. Thus,  $\bar{\delta}(\beta)$  is able to quantify the observation that patterns of Fig. 2 are more disordered than those of Fig. 1.

Next, we provide evidence to substantiate the claim that  $\bar{\delta}(\beta)$  are intensive variables for labyrinthine patterns such as those shown in Figs. 1 and 2 [35]. This is done by comparing values of  $\bar{\delta}(\beta)$  for patterns (with periodic boundary conditions) of several sizes. The sizes of the domains chosen are  $36\pi \times 36\pi$ ,  $36\pi \times 72\pi$ ,  $72\pi \times 72\pi$ , and  $144\pi \times 144\pi$ , and each pattern is generated by integrating a random initial state (with amplitude between  $\pm 10^{-2}$ ) for a time  $T = 8000$  under the SHE. The results, shown in Figure 5, give the mean of 10 patterns for each domain size (except the largest where only 5 patterns were used). The results indicate that  $\bar{\delta}(0.5)$ ,  $\bar{\delta}(1.0)$ , and  $\bar{\delta}(1.9)$  are intensive variables, and the corresponding  $\delta(\beta)$  are extensive variables.

## B. Relaxation of patterns

The characterization of textures using  $\bar{\delta}(\beta)$  finds one useful application in the study of the relaxation from an initially random state. Fig. 6 shows several snapshots of a relaxing pattern. During an initial period ( $t < T_0 \sim 800$ ) the local domains emerge out of the random background and the mean intensity  $\langle |u(\mathbf{x}, t)| \rangle$  nearly reaches its final value. The subsequent evolution due to domain coarsening is very slow. These qualitative features are repeated in multiple runs under the same control parameters.

Figure 7 shows the behavior of  $\Delta k$ ,  $\bar{\delta}(0.5)$ ,  $\bar{\delta}(1.0)$  and  $\bar{\delta}(1.9)$  for the evolution shown in Fig. 6. The curves remain identical (except for small statistical fluctuations) for different realizations of the experiment; i.e., the disorder function captures configuration independent aspects of the organization of patterns. The relaxation clearly consists of two stages, with a sharp transition in  $\bar{\delta}(\beta)$  at  $t = T_0$  [10,12].

FIG. 6. Several snap-shots of the relaxation of random initial state whose intensity is between  $\pm 10^{-2}$  under the SHE with  $D = 0.01$ ,  $\epsilon = 0.4$ ,  $\nu = 2$  and  $k_0 = 1/3$ . An initial phase ( $t < 800$ ) when the local striped patterns are being formed is followed by domain coarsening.

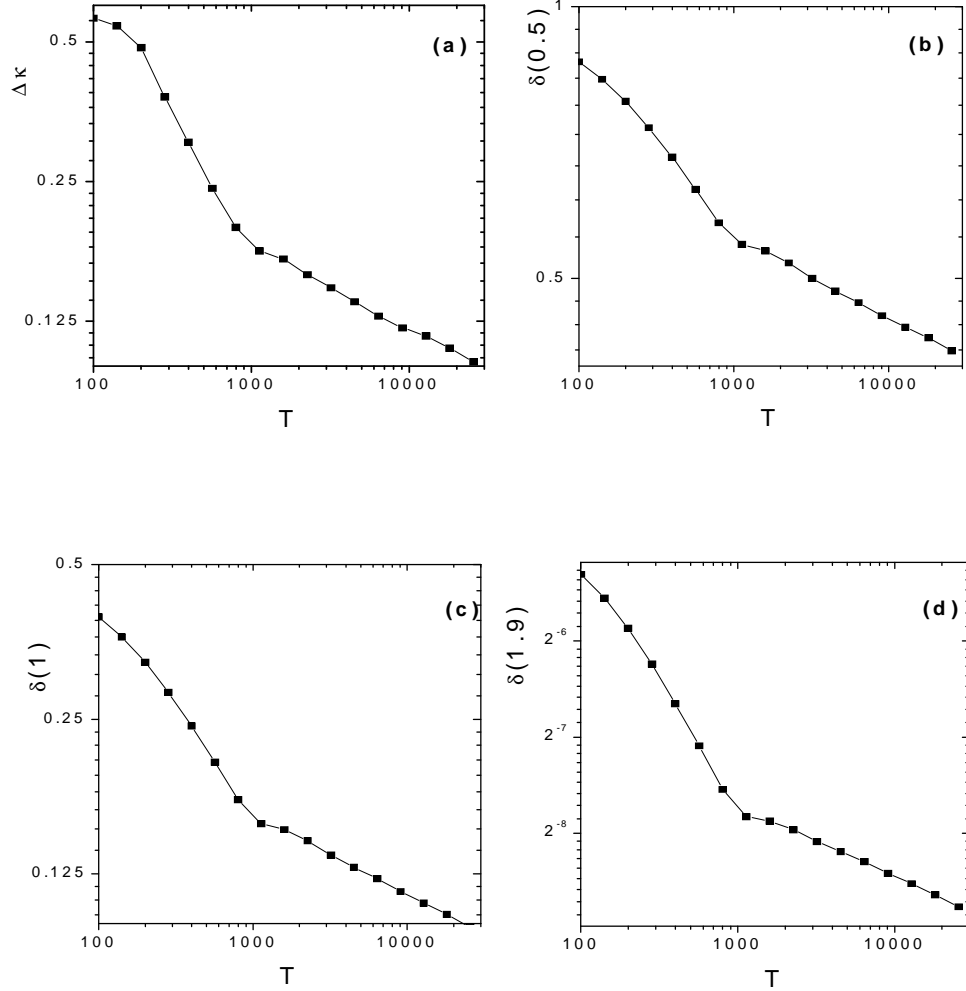


FIG. 7. The behavior of (a)  $\Delta k$ , (b)  $\bar{\delta}(0.5)$  (c)  $\bar{\delta}(1)$  and (d)  $\bar{\delta}(1.9)$  during the evolution shown in Fig. 6. During the initial phase  $\bar{\delta}(\beta)$  decays (approximately) like  $t^{-\frac{1}{2}\beta}$ . During the second phase the scaling is nontrivial; e.g.,  $\bar{\delta}(0.5) \sim t^{-0.09}$ ,  $\bar{\delta}(1.0) \sim t^{-0.15}$  and  $\bar{\delta}(1.9) \sim t^{-0.19}$ . The transition between the two phases occurs around  $t = 800$ .

During the initial phase, the time evolution of  $\bar{\delta}(1)$  changes smoothly from a logarithmic decay to a power law  $\bar{\delta}(1) \sim t^{-\gamma_1}$ , where  $\gamma_1 \approx 0.5$ . Corresponding  $t^{-\frac{1}{2}}$  de-

cay has been observed in the width of the structure factor [10]. The scaling is “trivial” in the sense that for other “moments”  $\bar{\delta}(\beta) \sim t^{-\frac{1}{2}\beta}$  [36]. The decay of  $\bar{\delta}(\beta)$  appears

to be associated with the  $L \sim t^{\frac{1}{2}}$  growth of domains in non-conserved systems [37].

The second phase of the relaxation (due to domain coarsening) exhibits a more complex behavior. The moments  $\bar{\delta}(0.5)$ ,  $\bar{\delta}(1)$  and  $\bar{\delta}(1.9)$  behave approximately as  $t^{-0.09}$ ,  $t^{-0.15}$  and  $t^{-0.20}$  respectively, indicating the presence of “non-trivial” scaling [13]. Since the relative contribution of isolated defects increases with  $\beta$  (Section II), the slower decay of  $\bar{\delta}(1.9)$  (compared to  $\bar{\delta}(1)^{1.9}$ ) suggests that changes in the density of defects is less significant than the reduction of curvature of the contour lines [10].

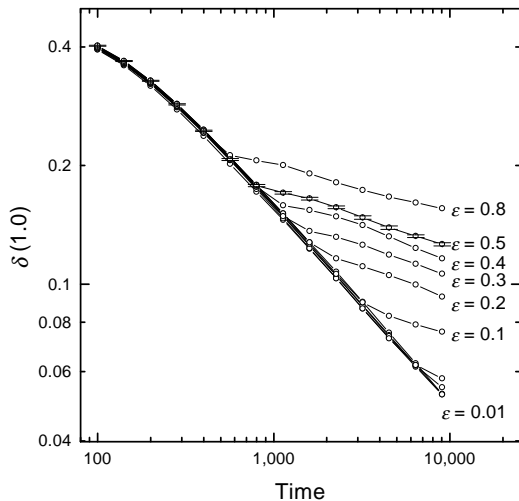


FIG. 8. The evolution of  $\bar{\delta}(1)$  for patterns generated by integrating random initial states under the SHE for several values of  $\epsilon$ . Each curve is an average of five runs. For clarity, the standard deviations are shown only for one parameter value. For distinct  $\epsilon$ ,  $\bar{\delta}(1)$  exhibits identical behavior during initial growth of domains, and decays at the same rate during the coarsening phase. The other moments  $\bar{\delta}(\beta)$  exhibit similar behavior.

### C. Changes in the relaxation with $\epsilon$

Figure 8 shows the behavior of  $\bar{\delta}(1)$  during the relaxation of random initial states under the SHE for several values of  $\epsilon$ , all other parameters being fixed. The initial decay of  $\bar{\delta}(1)$  and the rate of decay during the second phase are seen to be independent of  $\epsilon$ . Furthermore, the transition between the two phases advances with increas-

ing  $\epsilon$ . Similar results are observed for all values of the moments  $\beta$ .

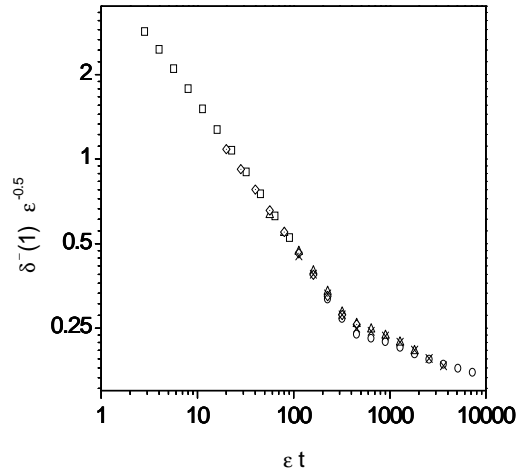


FIG. 9. The scaling function for the relaxation obtained by the rescaling  $t' = t\epsilon$  and  $\bar{\delta}' = \bar{\delta}\epsilon^{-\frac{1}{2}}$ . The data correspond to  $\epsilon$  values of 0.01, 0.05, 0.1, 0.4 and 0.8.

Suitable scaling of variables, including  $t \rightarrow \epsilon t$  can be used to eliminate  $\epsilon$  from the SHE. Hence we expect that the rescaling  $t \rightarrow \epsilon t$  and  $\bar{\delta}(1) \rightarrow \epsilon^{-\frac{1}{2}}\bar{\delta}(1)$  will lead to collapse of the curves shown in Fig. 8. This is indeed the case as seen from the scaling function (Fig. 9).

## V. RELAXATION IN NONVARIATIONAL SYSTEMS

In this Section we discuss properties of  $\bar{\delta}(\beta)$  when the spatio-temporal dynamics is nonvariational. The absence of an underlying “energy” of the dynamics suggests a faster relaxation, since the system cannot be constrained by “metastable states” during the evolution. The behavior of the disorder function confirms this expectation.

Figure 10 shows the behavior of  $\bar{\delta}(1)$  for the organization of a random field under a nonvariational SHE (i.e.,  $\nu \neq 0$ ). The decay of  $\bar{\delta}(1)$  remains the same (as the analogous variational dynamics) during the initial relaxation (Fig. 7) and becomes faster during the coarsening phase. As the coefficient  $\nu$  of the “nonvariational term” in Eqn. (6) increases (the value of the remaining coefficients remaining the same), so does the relaxation rate during the coarsening phase (Fig. 11).

The wave-number (obtained by minimizing  $\bar{\delta}(1)$  over  $k_0$ ) relaxes to a value ( $k_0 = 0.61$ ) that is larger than the corresponding one for the variational case ( $k_0 = 0.59$ ). Such a deviation was observed earlier in Ref. [12] where it was suggested that  $k_0$  (for the nonvariational case) corresponds to the zero-climb velocity of isolated dislocation defects.

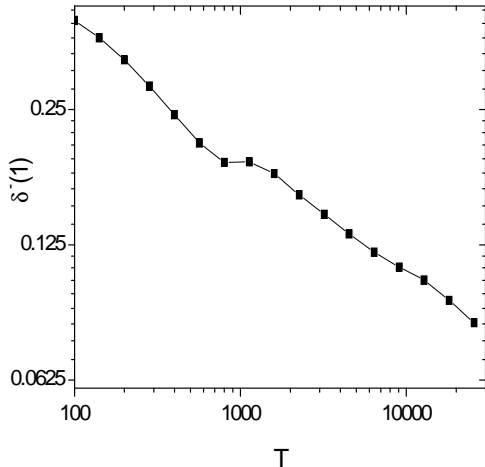


FIG. 10. The behavior of  $\bar{\delta}(1)$  for the evolution of a random initial state under the nonvariational modification of the SHE. The parameters of the SHE are the same as given in Fig. 6 except for  $\nu = 2.0$ . The initial decay is identical to the variational case while the coarsening phase exhibits a faster decay of  $\bar{\delta}(1)$ .

## VI. DISCUSSION

We have used the disorder function  $\bar{\delta}(\beta)$  to characterize properties of textured patterns and their relaxation from initially random states. The disorder function was defined by requiring its invariance under rigid motions of a single texture. It was found to be identical for multiple patterns generated under similar external conditions; i.e.,  $\bar{\delta}(\beta)$  is configuration independent. We provided evidence to confirm that the moments are intensive variables. In addition, the disorder function can differentiate between patterns with distinct characteristics.

The evolution of initially random states under the Swift-Hohenberg equation is conveniently described using  $\bar{\delta}(\beta)$ . The relaxation consists of two distinct stages separated by a sharp transition. During the initial phase,

local striped domains emerge out of the noisy background and their amplitudes saturate close to their final value. This behavior is described by a logarithmic decay followed by a power law decay of the disorder  $\bar{\delta}(1) \sim t^{-\frac{1}{2}}$ . The scaling is “trivial” in the sense that the decay of the remaining moments satisfy  $\bar{\delta}(\beta) \sim \bar{\delta}(1)^\beta$ . The second phase of the relaxation corresponds to domain coarsening and is a much slower process. The scaling during this phase is nontrivial.

As the system is driven further from the onset of patterns (as measured by the parameter  $\epsilon$ ) the duration of the initial phase is reduced. However, the rates of decay of the disorder function for the two phases remain unchanged and rescaling of time by  $\epsilon$  and of  $\bar{\delta}(\beta)$  by  $\epsilon^{-\frac{1}{2}\beta}$  leads to a scaling collapse.

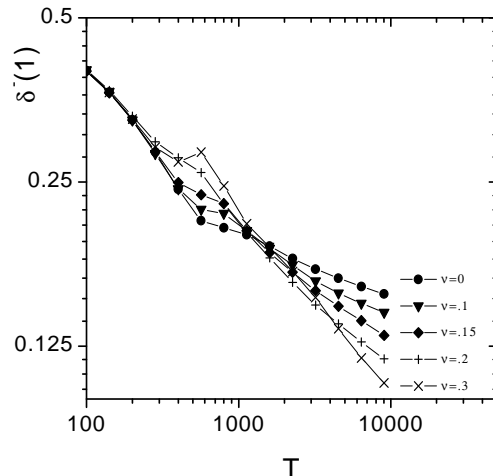


FIG. 11. The behavior of  $\bar{\delta}(1)$  for several values  $\nu$ . Observe that the decay during the growth phase remains the same, while the decay during the coarsening phase increases with  $\nu$ .

The addition of nonvariational terms to the spatio-temporal dynamics leads to several interesting observations. The decay of disorder during the initial phase is unchanged, and appears to be a model independent feature. Thus, one may expect to observe it during relaxation of patterns in experimental systems. The expectation of a faster relaxation in nonvariational systems (due to the absence of “potential minima”) is seen only during domain coarsening. This rate of relaxation is system dependent and increases as the coefficient of the nonvariational term.

There is very little theoretical understanding of the observed behavior of the disorder function. The decay of  $\bar{\delta}(\beta)$  during the initial phase of pattern relaxation is reminiscent of analogous behavior in the XY-model [38,39], and appears to correspond to the  $L \sim t^{\frac{1}{2}}$  growth of domains in nonconserved systems [37].

We would like to thank K. Bassler, D. K. Hoffman, R. E. Jones, D. J. Kouri and H. L. Swinney for many stimulating discussions. This work was partially funded by the Office of Naval Research and the Energy Laboratory at the University of Houston.

- 
- [1] Q. Ouyang and H. L. Swinney, *Nature (London)* **352**, 610 (1991).
- [2] M. S. Heutmaker and J. P. Gollub, *Phys. Rev. A* **35**, 242 (1987).
- [3] E. Bodenschatz, J. R. de Bruyn, G. Ahlers, and D. S. Cannel, *Phys. Rev. Lett.* **67**, 3078 (1991).
- [4] R. E. Rosenweig, *Ferrohydrodynamics* (Cambridge University Press, Cambridge, 1985).
- [5] F. Melo, P. Umbanhowar, and H. L. Swinney, *Phys. Rev. Lett.* **72**, 172 (1993).
- [6] M. C. Cross and P. C. Hohenberg, *Rev. Mod. Phys.* **65**(3), 851 (1993).
- [7] P. K. Jakobsen, J. V. Maloney, and A. C. Newell, *Phys. Rev. A* **45**, 8129 (1992).
- [8] M. Bestehorn, *Phys. Rev. E* **48**, 3622 (1993).
- [9] M. Golubitsky, I. Stewart, and D. G. Schaeffer, *Singularities and Groups in Bifurcation Theory* (Springer-Verlag, New York, 1988), Vol. 2.
- [10] K. R. Elder, J. Viñals, and M. Grant, *Phys. Rev. A* **46**, 7618 (1990).
- [11] Q. Ouyang and H. L. Swinney, *Chaos* **1**, 411 (1991).
- [12] M. C. Cross and D. I. Meiron, *Phys. Rev. Lett.* **75**, 2152 (1995).
- [13] J. J. Christensen and A. J. Bray, preprint (cond-mat/9804034).
- [14] Q. Hou, S. Sasa, and N. Goldenfeld, *Physica A* **239**, 219 (1997).
- [15] G. H. Gunaratne, R. E. Jones, Q. Ouyang, and H. L. Swinney, *Phys. Rev. Lett.* **75**, 3281 (1995).
- [16] G. H. Gunaratne, D. K. Hoffman, and D. J. Kouri, *Phys. Rev. E* **57**, 5146 (1998).
- [17] A. Kudrolli, B. Pier, and J. P. Gollub, "Superlattice Patterns on Surface Waves," to appear in *Physica D*.
- [18] S. L. Judd and M. Silber, "Simple and Superlattice Turing Patterns in Reaction-Diffusion Systems: Bifurcation, Bistability, and Parameter Collapse," Northwestern University preprint.
- [19] W. S. Edwards and S. Fauve, *Phys. Rev. E* **47**, R788 (1993).
- [20] D. Levine and P. J. Steinhart, *Phys. Rev. Lett.* **53**, 2477 (1984).
- [21] L. Landau and E. Lifshitz, *Fluid Mechanics*, Pergamon Press, Oxford, 1959.
- [22] M. C. Cross, *Phys. Rev. A* **25**, 1065 (1982).
- [23] D. K. Hoffman, M. Arnold, and D. J. Kouri, *J. Chem. Phys.* **96**, 6539 (1992).
- [24] D. K. Hoffman, G. H. Gunaratne, D. Z. Zhang, and D. J. Kouri, University of Houston preprint.
- [25] Y. Pomeau and P., Manneville, *Phys. Lett.* **75A**, 296 (1980).
- [26] In general  $\Delta k$  can be defined to be the distance between  $k$ -values for which  $\bar{\delta}(1)$  is a factor  $F$  ( $> 1$ ) of the minimum. Properties studied in the paper, such as the decay rates, are independent of  $F$ .
- [27] Y. Tu and M. C. Cross, *Phys. Rev. Lett.* **75**, 2152 (1995).
- [28] R. E. Jones, "Characterizing Disorder in Labyrinthine Patterns," Ph. D. Thesis, University of Houston (1997).
- [29] D.K. Hoffman, T.L. Marchioro, M. Arnold, Y. Huang, W. Zhu, and D.J. Kouri. *J. Math. Chem.* **20** 117 (1996).
- [30] D. K. Hoffman and D. J. Kouri. Proceedings of the Third International Conference on Mathematical and Numerical aspects of Wave Propagation, SIAM, 1995, pp. 56-83.
- [31] W. Zhu, Y. Huang, G. A. Parker, D. J. Kouri, and D. K. Hoffman. *J. Chem. Phys.* **98**, 12,516 (1994).
- [32] J. Swift and P. C. Hohenberg, *Phys. Rev. A* **15**, 319 (1977).
- [33] P. Gray and S. K. Scott, *Chem. Eng. Sci.* **38**, 29 (1983); *J. Phys. Chem.* **89**, 22 (1985).
- [34] W. H. Press, B. P. Flannery, S. A. Teukolsky and W. T. Vetterling, *Numerical Recipes - The Art of Scientific Computing* (Cambridge University Press, Cambridge, 1988).
- [35] The disorder function is not intensive for patterns with global regularity, such as a single target pattern or a single domain wall.
- [36] The behavior during the entire first stage can be approximated by  $\bar{\delta}(\beta, t) = 1/(a + b \log(t) + ct^{\beta/2})$ , for fixed  $a$ ,  $b$ , and  $c$ .
- [37] A. D. Rutenberg and A. J. Bray, *Phys. Rev. E* **51**, 5499 (1995).
- [38] K. Kawasaki, *Phys. Rev. A* **31**, 3880 (1985).
- [39] R. Loft and T. A. DeGrand, *Phys. Rev. B* **35**, 8528 (1987).

This figure "sh1.gif" is available in "gif" format from:

<http://arxiv.org/ps/patt-sol/9809001v1>

This figure "sh2.gif" is available in "gif" format from:

<http://arxiv.org/ps/patt-sol/9809001v1>

This figure "sh6.gif" is available in "gif" format from:

<http://arxiv.org/ps/patt-sol/9809001v1>